6th European Conference on Computational Mechanics (ECCM 6)
7th European Conference on Computational Fluid Dynamics (ECFD 7)
1115 June 2018, Glasgow, UK

COMPARISONS OF SYNTHETIC TURBULENCE MODELS USED IN A BEMT TIDAL TURBINE MODEL

MICHAEL TOGNERI[1], MATT EDMUNDS[1], IAN MASTERS[1], CLÉMENT CARLIER[2], CAMILLE CHOMA BEX[3] AND GRÉGORY PINON[3]

[1] College of Engineering, Swansea University, Swansea SA1 8EN, UK,
M.Togneri@swansea.ac.uk

[2] IFREMER, 150 Quai Gambetta, 62200 Boulogne s/ Mer, France

[3] Normandie University, UNIHAVRE, CNRS, LOMC, 76600 Le Havre, France

Key words: synthetic turbulence, blade element momentum theory, tidal turbines

Abstract. Turbulence in marine currents is a crucial factor governing both the peak loads and the magnitude of the fluctuating loads experienced by tidal energy converters (TECs) , and thus ultimately on the fatigue life of such devices and their components. In this paper, we use a low-cost blade element momentum theory (BEMT) model of a TEC to investigate turbulence effects. To complement the strengths of BEMT, it is best to incorporate turbulent flow conditions with low computational overhead: this motivates the use of synthetic turbulent methods. This broad family of methods generates velocity fields that are statistically equivalent to real turbulence, but not necessarily physical. This study uses the synthetic eddy method (SEM) and the Sandia method. We show that both methods indicate a straightforward relationship between the turbulence intensity and the magnitude of fluctuating loads.

1 INTRODUCTION

Turbulence is a significant concern for tidal energy converters (TECs), due to its importance in determining the fluctuating loads on turbine blades [1] and therefore on their fatigue life. Different studies have examined various turbulence parameters for characterising marine current turbulence (see for example [2, 3]), but no final consensus on the most crucial metrics has been reached. Nonetheless, it is intuitive that some measure of turbulence strength will be needed, and this is most often reported as turbulent kinetic energy (k) or turbulence intensity (TI). Aside from the problem of characterising turbulence, computational and experimental investigations into how to best translate turbulence to turbine are also ongoing [4, 5].

This paper presents results from blade element momentum theory (BEMT) simulations of a flume-scale tidal turbine. For use in conjunction with this turbine model, turbulence must be modelled in a way that plays to the strengths of BEMT: its ability to

quickly investigate a wide range of flow cases and operating conditions. A high-fidelity but computationally-expensive method for generating turbulent inflow conditions defeats the purpose of using BEMT in the first place. We are therefore motivated to employ synthetic turbulence methods, which create velocity fields that are statistically representative of real turbulence, but are not necessarily physically correct in the sense that the flowfields do not satisfy the Navier-Stokes equations. The two synthetic eddy methods investigated in this study are the synthetic eddy method (SEM) [6] and the spectral method (or Sandia method) [7]. SEM was originally developed to generate inflow conditions for large eddy simulations, and the Sandia method is widely employed in commercial codes such as *Tidal Bladed* and *TurbSim*.

We begin the paper with a brief sketch of the theory behind the turbine and turbulence models, and a description of the test case. We then show that the BEMT model is able to satisfactorily predict the performance of the model turbine in a non-turbulent reference flow, and go on to describe some key observations from simulations of the turbine with different turbulent inflow conditions.

2 BACKGROUND

2.1 Blade element momentum theory

The basic principal of BEMT is that a conventional horizontal-axis turbine can be regarded as both a momentum sink/source and a collection of quasi-2D blade elements whose hydrodynamic forces are governed by inflow velocity and flow direction. A suitable parametrisation of both theoretical models allows the difference between them to be characterised by two variables called the 'induction factors'; finding the value of the induction factors that minimises the difference allows us to uniquely determine the loads and momentum absorption of the turbine. The specific BEMT model employed in this study is a well-validated, robust code developed at Swansea [8, 9] that has several modifications to the classical formulation. Most importantly, it permits unsteady, non-uniform inflow conditions - this modification makes it possible to predict the turbine response to turbulence.

2.2 Synthetic eddy method

SEM creates a synthetic turbulent flowfield by populating a region of space with 'eddies' of specified shape, size and strength. By choosing appropriate values for these properties based on real turbulence measurements (e.g., turbulent kinetic energy, anisotropy ratios, integral lengthscales etc.), the resultant velocity field will have the same Reynolds stress tensor as the real velocity field whose measurements it is based on. A fuller description of the underlying mathematics is available in [6].

2.3 Sandia method

The Sandia method is based on velocity spectra. We select a grid of points in space for which we want to specify time series of turbulent velocity, then define an appropriate

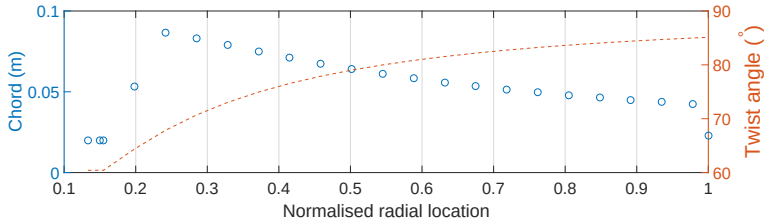

Figure 1: Radial chord and twist distributions for the rotor used in the case study. Twist is defined as the angle between the chord line and the axis of rotation.

spectrum for each point (based on real measurements or on canonical spectra such as the von Kármán spectrum) and cross-spectra for each pair of points. By applying a random phase to the spectra and transforming into the time domain, we obtain a randomised velocity field whose spectral properties statistically match those of the input data. More detail on the method can be found in [7]

2.4 Case study

To ensure that our results can be meaningfully validated, we simulate a case for which we have some experimental data. The case chosen was a lab-scale turbine that has been extensively tested in the IFREMER flume tank [10]. The rotor used in the experiments had a conventional three-bladed configuration of 0.7m diameter; its blade shape and twist distribution are shown in figure 1, and it used a NACA 63418 section for the entire blade length. Of the range of flow conditions examined in the IFREMER experiments, we restrict ourselves in the current study to simulating two cases, both with a mean flow velocity of 1ms^{-1}, which we denote simply the 'low turbulence' and 'high turbulence' cases. These cases are at 3% and 15% turbulence intensity (TI) respectively and correspond to the flume being operated with and without a flow-smoothing honeycomb upstream of the working section. In addition to the TI, we characterise turbulence by its anisotropy ratio, i.e., the relative proportion of turbulent energy due to fluctuations in different directions. Following the theoretical predictions of Nezu and Nakagawa [11], later corroborated by field measurements [1], we assume that this ratio takes the value $\sigma_u : \sigma_v : \sigma_w = 1 : 0.75 : 0.56$, where σ_u represents the standard deviation of the along-stream u-component of velocity.

3 RESULTS

3.1 Validation of BEMT for steady flow operation

To validate the ability of the BEMT model to accurately predict the turbine's performance, we compare the predicted performance curves against the measurements taken in [10]. The results can be seen in figure 2. There is very good agreement between model and experiment for the power coefficient C_P, but the model appears to underpredict the thrust coefficient C_T. This is explained, however, by the fact that the experimental measurements of thrust also include the drag on the turbine support structure.

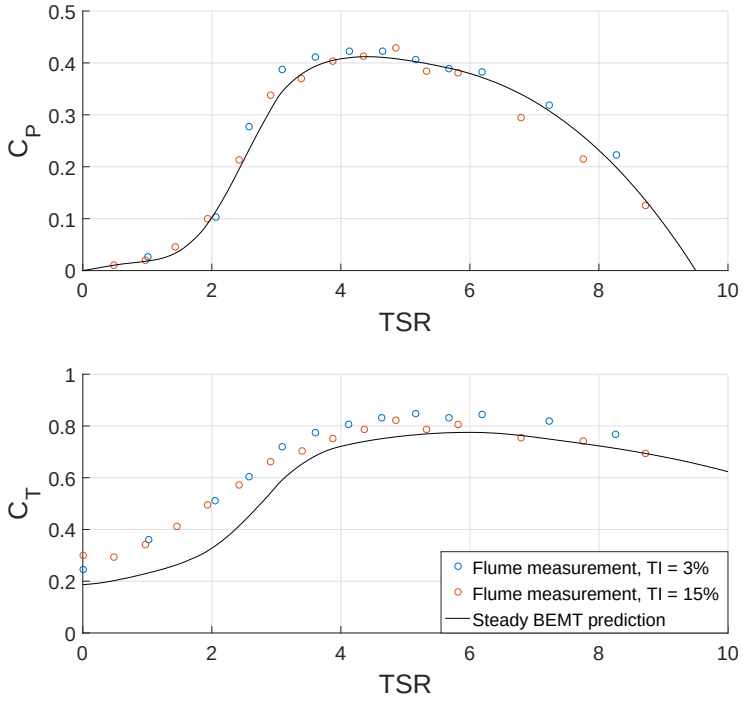

Figure 2: Power and thrust coefficient dependence on TSR. Flume data are taken from Mycek *et al.* [10] Experimental data points represent a time-average value over 100s of measurement.

3.2 Generation of the synthetic turbulent flowfields

Both synthetic turbulence models were used to realise 100 instances of the high-turbulence and low-turbulence velocity fields. Each realisation created a velocity field of size 10m in the streamwise direction (i.e., enough for 10s of flow at a mean flow speed of 1ms^{-1}), and 1.05m in both breadth and height (i.e., equal to the 1.5 times the diameter of the turbine). In table 3.1, the mean turbulent properties of these flowfields over all realisations are presented. For both models, the high and low turbulent cases are well-captured when examined in terms of the key parameters of TI and anisotropy ratio.

Table 1: Mean values and standard deviations of turbulence intensity (I_∞) and anisotropy ratio $\sigma_u : \sigma_v : \sigma_w$ for the SEM and Sandia methods compared to the benchmark turbulent flow cases

	I_∞	$\sigma_u : \sigma_v : \sigma_w$
Target	3%	$1 : 0.75 : 0.56$
SEM	$2.97 \pm 0.03\%$	$1 \pm 0.01 : 0.749 \pm 0.008 : 0.557 \pm 0.008$
Sandia	$3.00 \pm 0.05\%$	$1 \pm 0.01 : 0.747 \pm 0.010 : 0.557 \pm 0.005$
Target	15%	$1 : 0.75 : 0.56$
SEM	$14.8 \pm 0.1\%$	$1 \pm 0.03 : 0.750 \pm 0.012 : 0.558 \pm 0.013$
Sandia	$15.1 \pm 0.2\%$	$1 \pm 0.02 : 0.744 \pm 0.013 : 0.553 \pm 0.012$

3.3 Load coefficients in turbulent conditions

The effect of synthetic turbulence on the flume-scale turbine is illustrated in figure 3. The turbine is operated at a fixed tip speed ratio (TSR) relative to the mean velocity within the numerical model, and using this simple control scheme three different operating conditions are investigated. Specifically, we look at optimum operation (i.e., for a TSR value of 4.4, at which C_P reaches its maximum, cf. figure 2) as well as operation in the stall region (TSR 2.5) and the overspeed region (TSR 8). It is immediately clear from this figure that increasing the turbulence intensity causes a greater variability in the mean load coefficients. In fact, we find that the increase in coefficient standard deviation is almost exactly proportional to the increase in TI. As we move from the low turbulence to the high turbulence flow (a fivefold increase in TI), the standard deviations of the load coefficients increase by a value in the range 4.6-5.8.

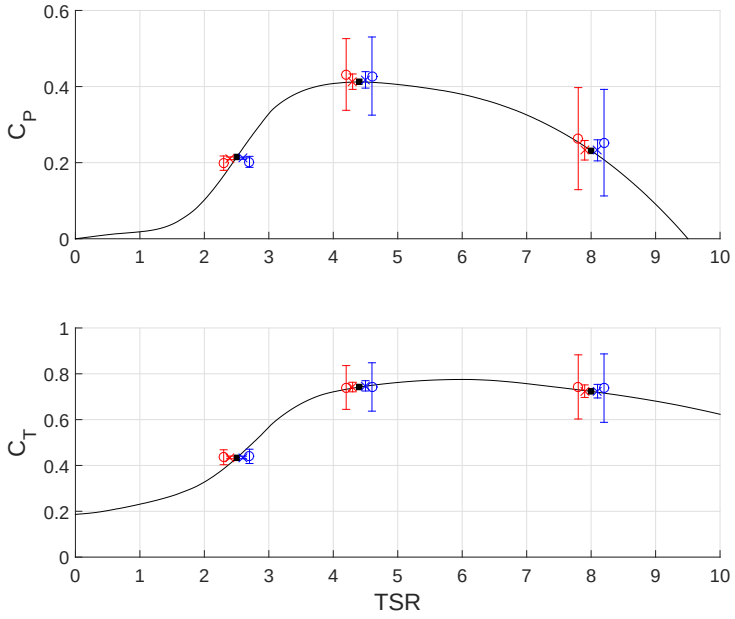

Figure 3: Power and thrust coefficients for turbulent simulations, compared to TSR-coefficient curves for steady flow. Black squares indicate the stall, optimum and overspeed operating cases; coloured markers show mean coefficient values for turbulent cases with error bars indicating standard deviation. Red markers and bars correspond to SEM turbulence, blue to Sandia turbulence; crosses indicate coefficients calculated for turbulence intensity of 3% and circles indicate those calculated for turbulence intensity of 15%.

3.4 Angle of attack and load distributions

The most striking result from figure 3 is that the load coefficients are much less variable in stall than they are in optimum or overspeed operation. This is a counterintuitive; see section 4 for a more in-depth discussion of this point. To ensure that this result is

not erroneous, we examine the force variability in more detail by looking at the radial distributions of thrust and in-plane force. In order to make sense of these force distributions, however, we first examine the distribution of angle of attack, as shown in figure 4.

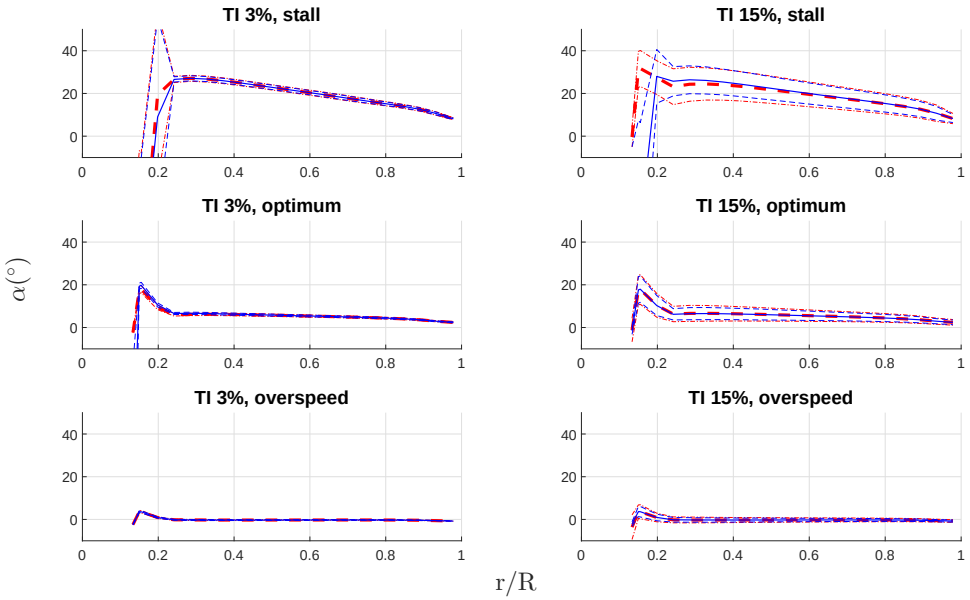

Figure 4: Distributions of angle of attack on turbine blades, averaged across all blades and all runs. Average values obtained using SEM turbulence are shown as a dashed red line, with a dash-dot line indicating standard deviation about the average. Average values obtained using Sandia turbulence are shown as a solid blue line, with a dashed line indicating standard deviation.

The results in this figure indicate that, as expected, the angle of attack varies more widely in stall than in optimum or overspeed operation. Furthermore, in stall operation there is a significant proportion of the blade span that is at angle of attacks above stall (ca. 14°). However, this increased variability is not in evidence when we look at the distribution of forces on the blades, as seen in figures 5 and 6. Note that the forces are shown per unit length in the radial direction, in order to prevent distortion of the results due to the different radial sizes of the blade elements in the BEMT representation of the rotor.

4 DISCUSSION

The most surprising result presented in section 3 is that turbine load coefficients are predicted to vary less significantly in stall than in optimum or overspeed operation, as illustrated in figure 3. This is the opposite of what we would expect intuitively for two reasons. Firstly, a blade operating near stall will see its angle of attack vary more widely for the same turbulent fluctuations, as the low TSR of stall operation means that the inflow variation is more significant in comparison to the rotational velocity and so the

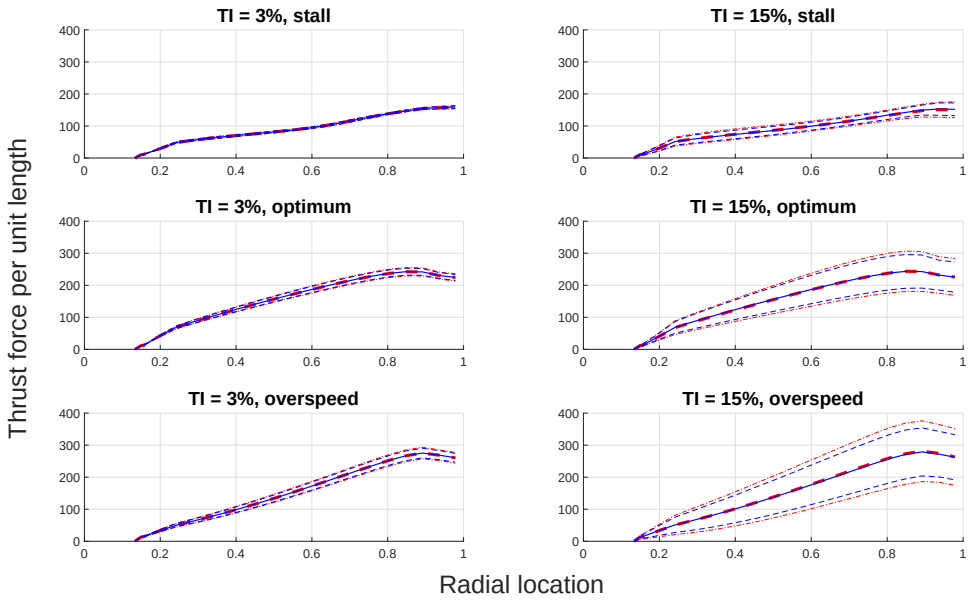

Figure 5: Distributions of thrust force per length on turbine blades, averaged across all blades and all runs. Average values obtained using SEM turbulence are shown as a dashed red line, with a dash-dot line indicating standard deviation about the average. Average values obtained using Sandia turbulence are shown as a solid blue line, with a dashed line indicating standard deviation.

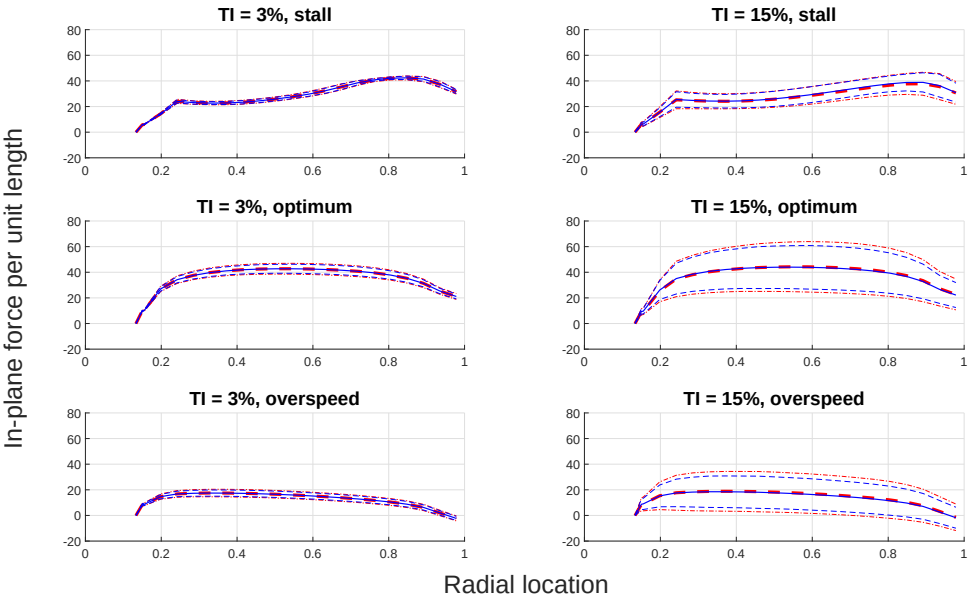

Figure 6: Distributions of in-plane force per length on turbine blades, averaged across all blades and all runs. Average values obtained using SEM turbulence are shown as a dashed red line, with a dash-dot line indicating standard deviation about the average. Average values obtained using Sandia turbulence are shown as a solid blue line, with a dashed line indicating standard deviation.

same velocity flowfield will yield greater variability in angle of attack. Secondly, these angle of attack fluctuations will more frequently taking the blade in and out of a stalled condition, and in the absence of a dynamic stall model there is nothing to smooth these transitions.

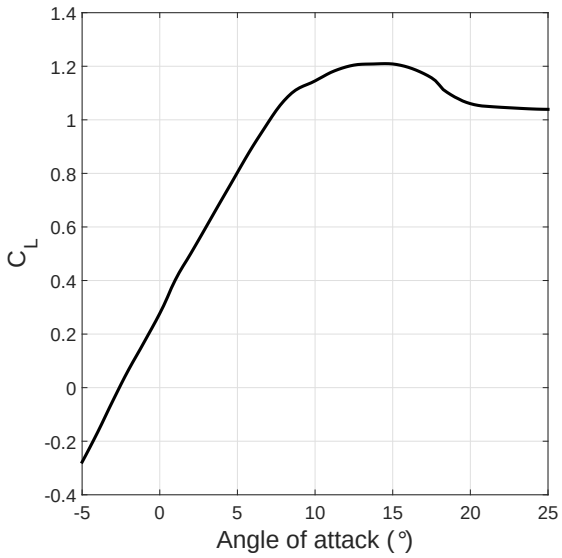

Figure 7: Lift coefficient of the NACA 63418 blade section, plotted against angle of attack for a selected range of angle of attack values encompassing stall. Data taken from [12]

We have shown in figure 4 that the expected angle of attack behaviour is indeed observed in the simulations; nonetheless, the corresponding hydrodynamic forces on the blades, as seen in figures 5 and 6 still exhibit bevaviour contrary to this. We have checked that there is no error in the simulations by recalculating the hydrodynamic forces based only on the blade geometry, and have confirmed that the force and angle of attack results agree with one another. A possible explanation may be found in the lift coefficient behaviour of the NACA 63418 blade section used in the IFREMER turbine, which is depicted in figure 7. This shows that the stall behaviour of this section is comparatively gentle, without a large drop in lift after separation at approximately 14°. Thus, in stall operation, the variability of the forces resulting from the relatively wide angle of attack range is plausibly smaller than that in optimum or overspeed operation. Furthermore, we can be confident that this is a realistic picture of the lift and drag behaviour of the blade section because the steady-flow case has been well validated against experimental measurements, as seen in figure 2.

It is also interesting that the variability of the force coefficients is almost directly proportional to the level of turbulence intensity in the flow. While it would be too hasty to definitively conclude that this is the case from the two data points presented here (i.e.,

the low and high turbulence cases), the data shown indicates that we may be able to rely on a very straightforward relationship between turbulence intensity and load variability: specifically, they are directly proportional, such that a doubling of TI will result in a doubling of the standard deviation of the turbine load coefficients.

Lastly, we observe that there is little noticeable difference between the simulations carried out with SEM turbulence and those carried out with Sandia turbulence. There is no significant change in mean results when switching between the two turbulence models, although the variability of the loads is somewhat affected: the standard deviations of the load coefficients differ by approximately 10% on average, while distributed load standard deviations differ by approximately 20% on average. This discrepancy is probably attributable to differences in the variability of the velocity fields across the rotor disc. There is no experimental data against which we can validate the results relating to load variability, so we cannot make a choice on this basis. There is therefore little reason to recommend the use of one model over another at this juncture.

5 CONCLUSIONS

We have tested the ability of a BEMT model to predict load variability on a turbine when it experiences two forms of synthetic turbulence. We first demonstrated that the numerical model adequately predicts the turbine in steady conditions by validating it against laboratory results, and showed that the synthetic turbulence models could produce velocity flowfields that accurately captured the most important statistical parameters of the turbulence observed in the experimental studies. Following this, we simulated the turbine's response to several instances of the turbulent flow using both synthetic turbulence models in three different operating conditions (stall, optimum and overspeed). The results of these simulations indicated that the variability of turbine loads, as indicated by the load coefficients, is directly proportional to the turbulence intensity. We also observed that, counterintuitively, load variability is lower in stall than in other operating conditions. We verified that, despite this unintuitive result, stall operation is indeed associated with higher angle of attack variability, as expected. This unusual result is likely related to the relatively gentle stall of the NACA 63418 foil.

6 ACKNOWLEDGEMENTS

The authors acknowledge the financial support of the Welsh Assembly Government and Higher Education Funding Council for Wales through the Sêr Cymru National Research Network for Low Carbon, Energy and Environment. The work was also supported by the EPSRC-funded projects "Extension of UKCMER Core Research, Industry and International Engagement" (EP/M014738/1) and "SURFTEC" (EP/P008682/1), as well as the Interreg Atlantic Area project MONITOR (EAPA_333/2016). Clément Carlier would like to thank the Normandy Regional Council and IFREMER for the financial support of his Ph.D. grant. Camille Choma Bex acknowledges the financial support of IFREMER for her Ph.D. grant. The authors also would like to thank the CPER-ERDF program

NEPTUNE also financed by the Normandy Regional Council.

REFERENCES

[1] I.A. Milne, A.H. Day, R.N. Sharma and R.G.J. Flay, The characterisation of the hydrodynamic loads on tidal turbines due to turbulence. *Renew. Sust. Energ. Rev.*, Vol. **56**, pp. 851–864, 2016

[2] J. Thomson, B. Polagye, V. Durgesh and M.C. Richmond, Measurements of turbulence at two tidal energy sites in Puget Sound, WA. *IEEE Journal of Oceanic Engineering*, Vol. **37**(3), pp. 363–374, 2012

[3] M. Togneri and I. Masters, Micrositing variability and mean flow scaling for marine turbulence in Ramsey Sound. *Journal of Ocean Engineering and Marine Energy*, Vol. **2**(1), pp. 35–46, 2016

[4] T. Stallard, R. Collings, T. Feng and J. Whelan, Interactions between tidal turbine wakes: experimental study of a group of three-bladed turbines, *Philosophical Transactions of the Royal Society A*, Vol. **371**(1985)

[5] P. Pyakurel, J.H. VanZwieten, M. Danhak and N. Xiros, Numerical modeling of turbulence and its effect on ocean current turbines, *International Journal of Marine Energy*, Vol. **17**, pp. 84–97, 2017

[6] N. Jarrin, S. Benhamadouche, D. Laurence and R. Prosser, A synthetic-eddy-method for generating inflow conditions for large eddy simulations. *International Journal of Heat and Fluid Flow*, Vol. **27**(4), pp. 585–593 (2006)

[7] P. Veers, Three-dimensional wind simulation. *Sandia National Labs technical report* (1988)

[8] I. Masters, J. Chapman, J. Orme and M. Willis, A robust blade element momentum theory model for tidal stream turbines including tip and hub loss corrections. *Proc. IMarEST Part A - J. Mar. Eng. Tech.*, Vol. **10**(1), pp. 25–35, 2011

[9] J.C. Chapman, I. Masters, M. Togneri and J.A.C. Orme. The Buhl correction factor applied to high induction conditions for tidal stream turbines. *Renewable Energy*, Vol. **60**, pp. 472–480 (2013)

[10] P. Mycek, B. Gaurier, G. Germain, G. Pinon and E. Rivoalen. Experimental study of the turbulence intensity effects on marine current turbine behaviour, part I: One single turbine. *Renewable Energy*, Vol. **66**, pp. 729–726 (2014)

[11] I. Nezu and H. Nakagawa. Turbulence in open-channel flows, *Taylor & Francis* (1993)

[12] I.H. Abbott and A.E. von Doenhoff. Theory of wing sections, including a summary of airfoil data, *Courier Corporation* (1959)